Dynamics of particulate and dissolved organic and inorganic phosphorus during the peak and declining phase of an iron-induced phytoplankton bloom in the eastern subarctic Pacific

Takeshi Yoshimura[1,*], Jun Nishioka[2], Hiroshi Ogawa[3], Atsushi Tsuda[3]

[1]Central Research Institute of Electric Power Industry, 1646 Abiko, Abiko, Chiba 270-1194, Japan

[2]Institute of Low Temperature Science, Hokkaido University, Sapporo, Hokkaido 060-0819, Japan

[3]Atmosphere and Ocean Research Institute, The University of Tokyo, 5-1-5 Kashiwanoha, Kashiwa, Chiba 277-8564, Japan

*Corresponding author (present address): T. Yoshimura (yoshimura-t@fish.hokudai.ac.jp)

Faculty of Fisheries Sciences, Hokkaido University

Graduate School of Environmental Science, Hokkaido University

Kita 10, Nishi 5, Kita-ku, Sapporo, Hokkaido 060-0810 JAPAN

Tel: +81-11-706-2324

April 26, 2017 (submitted)

August 4, 2017 (resubmitted)

Submitted as a Research Paper to Journal of Marine Systems

ABSTRACT

Phosphorus (P) is an essential element for all organisms and thus the P cycle plays a key role in determining the dynamics of lower trophic levels in marine ecosystems. P in seawater occurs conceptually in particulate and dissolved organic and inorganic (POP, PIP, DOP, and DIP, respectively) pools and clarification of the dynamics in these P pools is the basis to assess the biogeochemical cycle of P. Despite its importance, behaviors of each P pool with phytoplankton dynamics have not been fully examined. We measured the four operationally defined P pools (POP_{op}, PIP_{op}, DOP_{op}, and SRP) during an iron-induced phytoplankton bloom (as part of the subarctic ecosystem response to iron enrichment study (SERIES)) in the eastern subarctic Pacific in summer 2002. During our observations of the iron-enriched patch from day 15 to day 26 after the iron infusion, chlorophyll-*a* concentration in the surface layer decreased from 6.3 to 1.2 μg L^{-1}, indicating the peak through decline phase of the phytoplankton bloom. At the bloom peak, P was partitioned into POP_{op}, PIP_{op}, and DOP_{op} in proportions of 60, 27, and 13 %, respectively. While chlorophyll-*a* and POP_{op} showed similar temporal variations during the declining phase, PIP_{op} showed a different peak timing with a 2 day delay compared to POP_{op}, resulting in a rapid change in the relative proportion of PIP_{op} to total particulate P (TPP = POP_{op} + PIP_{op}) at the peak (25 %) and during the declining phase of the bloom (50 %). A part of POP_{op} was replaced by PIP_{op} just after slowing down of phytoplankton growth. This process may have a significant role in the subsequent regeneration of P. We conclude that measurement of TPP alone is insufficient to show the interaction between P and phytoplankton dynamics and fractionation of TPP into POP_{op} and PIP_{op} provides useful insights to clarify the biogeochemical cycle of P.

Keywords:

Phosphorus

Organic matter

Inorganic matter

Phytoplankton bloom

1. Introduction

Phosphorus (P) is a factor regulating phytoplankton productivity in the ocean. Better understanding of the biogeochemical cycle of P is required to evaluate the role of P in controlling marine ecosystems and thus to determine the link with other bioactive elements such as carbon (C) and nitrogen (N). However, comprehensive studies on P are few compared with C and N (Karl, 2014). P in seawater occurs in both particulate and dissolved pools, and each of which contain organic and inorganic forms (POP, PIP, DOP, and DIP). Although the most favorable form of P for phytoplankton growth is orthophosphate (PO_4), recent studies have shown that other forms of P also play roles in the P cycle (Dyhrman, 2016; Karl, 2014). Since these different P pools would have different regeneration pathways and thus have different turnover times (Björkman and Karl, 2003), information on the size and dynamics of each P pool is necessary to characterize the P cycle. However, fractionated analyses of total particulate P (TPP) and total dissolved P (TDP) pools are scarce, as pointed out in Labry et al. (2013) and Karl and Björkman (2015), respectively.

Past studies have shown that the fractionated measurement of P is a strategy for a better understanding of the P cycle (Loh and Bauer, 2000). TPP pool can be operationally differentiated into HCl-extractable P and non-extractable P pools, and TDP pool can be differentiated into soluble reactive P (SRP) and soluble non-reactive P (SNP) pools; P pool can be fractionated into four operationally defined fractions using filtration and chemical fractionation methods, and these P pools have been assumed to represent PIP, POP, DIP, and DOP, respectively (Loh and Bauer, 2000). The pool size and relative composition of each fraction vary horizontally and vertically (Loh and Bauer, 2000; Piper et al., 2016; Yoshimura et al., 2007). Uncoupled behavior of POP and PIP in sinking particles was also reported in Benitez-Nelson et al. (2004). Recent P fractionation studies in estuarine (Labry et al., 2013; Lin et al., 2013) and Arctic waters (Lin et al., 2012; Piper et al., 2016) provide insights into the dynamics among the different P pools. Asahi et al. (2014) has shown that the POP to PIP ratio is a useful index to determine the origin of suspended particulate matter in the coastal environment. Although very detailed fractionation methods for TPP (Cade-Menun and Paytan, 2010; Miyata and Hattori, 1986; Ruttenberg, 1992) and TDP pool (Kolowith et al., 2001; Young and Ingall, 2010) have been developed, these studies have shown relatively simple fractionation techniques to be useful for a better understanding of the P cycle, especially when large amounts of samples are difficult to obtain notably in open ocean waters.

An issue is that chemically fractionated P pools are operationally defined pools and

do not necessarily correspond to the conceptual P pools (Fig. 1). As a typical DIP species, PO_4 has been measured by the molybdenum blue colorimetric method. However this method does not measure polyphosphates but does measure some part of acid-labile DOP. Thus the P fraction measured using the molybdenum blue technique does not represent DIP and is termed SRP (Benitez-Nelson, 2000). Although the difference between TDP and SRP has been assumed to be DOP, this fraction contains polyphosphates, and thus this P fraction should be termed as SNP (Benitez-Nelson, 2000). Similarly is the case for TPP fractionations. For suspended particulate matter samples on glass fiber filters, Labry et al. (2013) concluded that the high temperature combustion and acid hydrolysis method for TPP of Solórzano and Sharp (1980) and the acid hydrolysis method for PIP of Aspila et al. (1976) are the best methods to estimate the POP and PIP pools. However, since polyphosphate is only partially hydrolyzed (41−49 %) by the method of Aspila et al. (1976) (Labry et al., 2013), intracellular polyphosphates are significantly underestimated in PIP_{op} pools and included in POP_{op} pools (Fig. 1). Therefore we hereafter term the four operationally fractionated P pools as PIP_{op}, POP_{op}, SRP, and DOP_{op}. Care is required to discuss chemically fractionated P data with conceptual P pools, but simple chemical fractionations still have an advantage to obtain useful insights for a better understanding of the marine P cycle.

A phytoplankton bloom is a typical platform to study the dynamics of bioactive elements with the rapid buildup of phytoplankton biomass. Although C and N dynamics have been directly measured during phytoplankton blooms (Biddanda and Benner, 1997; Carlson et al., 2000; Wetz and Wheeler, 2003); P fractionated studies are scarce. We reported DOP_{op} production and decomposition during phytoplankton blooms in the subarctic Pacific (Yoshimura et al., 2014), but the dynamics of fractionated particulate P pools have not received sufficient research attention to enable a clearer understanding of P biogeochemistry. Fractionations of particulate P may be a key strategy to understand why P is preferentially regenerated from particulate materials produced by phytoplankton relative to C and N (Engel et al., 2002; Paytan et al., 2003; Yoshimura et al., 2009). Observations for the relationship between the temporal dynamics of different P pools and that of phytoplankton will provide insights to improve our understanding of the role of P in the marine environment.

The present study focused on measuring the dynamics of the four P pools during a model phytoplankton bloom in the open ocean. This study was conducted during a mesoscale in situ iron (Fe) enrichment experiment in the eastern subarctic Pacific, subarctic ecosystem response to iron enrichment study (SERIES). This was the first experiment to demonstrate the

dynamics of an Fe induced phytoplankton bloom from its evolution through to its termination during the 26-day observation using data from three research vessels (Boyd et al., 2004). We observed the phytoplankton bloom aboard the F.R.V. *Kaiyo-Maru* from day 15 to day 26, which corresponded to the peak and decline phase of the phytoplankton bloom (Saito et al., 2006). We discuss temporal variations of the four operationally defined P pools of PIP_{op}, POP_{op}, SRP, and DOP_{op} with that of the phytoplankton biomass in terms of chlorophyll-*a* (Chl-*a*) concentrations during the peak and decline phases of the SERIES phytoplankton bloom.

2. Materials and methods

2.1. SERIES experiment

A mesoscale in situ Fe enrichment experiment (SERIES) was conducted in the Alaskan gyre of the eastern subarctic Pacific (50.14°N, 144.75°W), north west of Ocean Station Papa, from 9 July to 4 August 2002 by R.Vs. *J.P. Tully*, *El Puma*, and *Kaiyo-Maru* (Boyd et al., 2004). Dissolved Fe (387 kg of Fe as $FeSO_4$) and the inert tracer SF_6 were injected into the surface mixed layer over an area of 8.5 × 8.5 km from the *J.P. Tully* on 9 July 2002 (denoted as day 0). The Fe infusion increased the in situ concentration of dissolved Fe from < 0.1 nmol L^{-1} to > 1 nmol L^{-1} (Boyd et al., 2004). A second release of dissolved Fe (102 kg of Fe) without SF_6 was conducted aboard the *J.P. Tully* in response to the declining dissolved Fe levels on 16 July 2002 (day 7), increasing the in situ concentration of dissolved Fe to ~0.6 nmol L^{-1} (Boyd et al., 2004). The Fe enriched patch was tracked by elevated SF_6 (until day 13) or decreased fCO_2 (after day 15) for 26 days (Law et al., 2006).

2.2. Field samplings

Seawater samplings for the fractionated P measurements were conducted inside (IN-patch) and outside (OUT-patch) the Fe enriched patch during days 15−26 aboard the *Kaiyo-Maru*. Samples for P fractionations were not obtained during days 0−14 during the observations of the other vessels. The positions of IN- and OUT-patch stations were determined to verify the center of the patch and outside the patch, respectively, by nighttime horizontal patch surveys (Law et al., 2006). Since the samples collected from OUT-patch were not traced with SF_6, we mainly focus on the IN-patch data. Discrete water samples were collected at predetermined depths (2, 5, 10, 20, 30, 50, 75, 100, 125, 150, and 200 m) in 10 L

Niskin-X bottles attached on a Kevlar wire or 12 L Niskin-X bottles attached to a CTD-carousel multiple sampler system. For dissolved P, subsamples were drawn from the Niskin bottles by gravity-filtration through an in-line 47 mm Whatman GF/F filter (precombusted at 450 °C for 4 h), attached directly to the Niskin bottle's spigot. The filtered subsamples were collected in acid-cleaned polypropylene bottles, and stored at −20 °C until analysis on land. For particulate P analysis, subsamples (600−3000 mL aliquots) were filtered through duplicate precombusted and acid-washed 25 mm GF/F filters under gentle vacuum at < 0.01 MPa; one for TPP and one for PIP_{op}. After the filtrations, the filters were washed with 0.17 mol L^{-1} Na_2SO_4 (Solórzano and Sharp, 1980), and stored at −20 °C until analysis on land. For Chl-*a* analysis, subsamples (116 mL aliquots) were filtered through 25 mm GF/F filter under gentle vacuum, and the Chl-*a* on the filter was extracted immediately with 90 % acetone at 4 °C in the dark for 24 h.

2.3. Chemical analyses

P concentrations were measured for four operationally defined pools, DOP_{op}, SRP, POP_{op} and PIP_{op}. The concentration of DOP_{op} was estimated as the difference between total dissolved P (TDP) and SRP concentrations. SRP was measured manually by the molybdenum blue method (Hansen and Koroleff, 1999) using a 50 mm path length quartz cell and a spectrophotometer (U-2001, Hitachi). The calibration was performed using KH_2PO_4 (Suprapur, Merck). Samples for the TDP analysis were autoclaved in an acid potassium persulfate (N and P analysis grade, Wako) solution at 123 °C for 120 min (Hansen and Koroleff, 1999; Ridal and Moore, 1990). TDP concentrations were measured as SRP after removing excess free chlorine by placing the samples in a hot water bath for 2 h. Analyses for SRP and TDP were done in triplicate for each sample, and the mean ± 1 standard deviation (SD) was reported for SRP and DOP_{op}. The detection limit for SRP and TDP, given as three times the standard deviation of 10 blank measurements, was 0.01 µmol L^{-1}. Accuracy of our SRP measurements was confirmed using reference materials for nutrients (Aoyama et al., 2012). The precision of the DOP_{op} concentration for a single sample analysis was typically ± 0.02 µmol L^{-1} (ranging ± 0.00 µmol L^{-1} to 0.04 µmol L^{-1}). Although we cannot evaluate the accuracy of our DOP_{op} measurements due to a lack of appropriate RMs for DOP_{op} analysis (Yoshimura, 2013), a good comparability in our analytical results was confirmed with stable DOP_{op} results (± 0.01 µmol L^{-1}) of the successive measurements of a batch of aged surface seawater sample (Yoshimura and Sharp, 2010). Coefficient of variance for DOP_{op} analysis

was 0−23 % for 0−50 m depth samples (roughly > 0.10 μmol L^{-1}) and 0−100 % for 75−200 m depth samples (roughly < 0.10 μmol L^{-1}). TPP was measured as SRP after high-temperature combustion and acid hydrolysis of the filter samples as described by Solórzano and Sharp (1980). PIP_{op} was extracted from filter samples with 1 N HCl at 20 °C in the dark for 24 h and quantified as SRP (Aspila et al., 1976). Analyses for TPP and PIP_{op} were done on single samples that were analyzed in duplicate and the mean ± range is reported. POP_{op} concentrations were calculated as the difference between TPP and PIP_{op}. A higher precision (± < 1 nmol L^{-1}) was obtained for TPP and PIP_{op} analyses due to the ca. 30 fold concentration factor used in the analytical procedure. Please note that these operationally defined P pools (PIP_{op}, POP_{op}, SRP, and DOP_{op}) do not necessarily correspond to the conceptual P pools (PIP, POP, DIP, and DOP).

Chl-*a* concentrations were measured onboard with a fluorometer (Model 10-AU, Turner Designs) with the acidification method of Holm-Hansen et al. (1965). Temporal changes in vertical profiles of Chl-*a* have already been presented in Saito et al. (2006).

3. Results and discussion

3.1. Development and decline of the SERIES phytoplankton bloom

As demonstrated in Saito et al. (2006), our observations during days 15−26 corresponded to the peak on day 17 and thereafter the declining phase of the phytoplankton bloom. The SERIES experiment started with a maximum surface Chl-*a* concentration of 0.3 μg L^{-1} before Fe enrichment (Marchetti et al., 2006). The surface Chl-*a* concentration reached 6.3 μg L^{-1} on day 15 and then decreased to 1.2 μg L^{-1} on day 26 in our observation in the IN-patch, indicating the development and decline of an Fe-induced phytoplankton bloom in contrast to the lower Chl-*a* concentrations in the OUT-patch (0.4−0.5 μg L^{-1} with occasionally high values of 1.8 μg L^{-1} on day 12 and 1.7 μg L^{-1} on day 26). Temporal changes in Chl-*a* concentration occurred in the upper 50 m layer (Fig. 2a), thus the bloom dynamics can be shown as the changes in inventories in 0−50 m depth for Chl-*a* as well as P pools. This corresponds to the variation of upper mixed layer depth (10−38 m) during days 2−19 (Marchetti et al., 2006) and of the main pycnocline (30−45 m) during our observation (Saito et al., 2006). When the data obtained by Institute of Ocean Sciences (IOS), Fisheries and Oceans Canada (F.A. Whitney, Personal communication) were combined with our data, the Chl-*a* inventory integrated for 0−50 m depth in the IN-patch was shown to have gradually

increased and peaked on day 17, and then decreased until day 26 (Fig. 3a).

The SERIES bloom was terminated by simultaneous limitation of diatom growth by both Fe and silicic acid (Boyd et al., 2005). Boyd et al. (2005) showed that Fe limitation was detected on day 13 and silicic acid depletion was observed by day 17. On the other hand, surface SRP concentrations decreased from 1.3 μmol L^{-1} on day 0 to 0.5 μmol L^{-1} on day 19 in the IN-patch (Fig. 2e) and ranged 0.9−1.2 μmol L^{-1} in the OUT-patch, indicating P sufficient conditions throughout the experiment even at the peak of the bloom. SRP inventory for 0−50 m depth decreased with the Chl-*a* increase and then increased toward an initial level in our observation in the IN-patch (Fig. 3b). Although bacterial activities will have played a role for the rapid increase in the SRP inventory during the declining phase, data on bacterial processes reported are available only until day 19 (Hale et al., 2006). Unlike with Chl-*a*, SRP inventories were not distinguishable between IN and OUT-patch before our observation (Fig. 3b). This is explained by the intrusion of a high nutrient water mass beneath the surface mixed layer of the IN-patch (Timothy et al., 2006), which was also detected in our SRP vertical profiles (Fig. 2e). Our data confirmed that phytoplankton grew under conditions that were not limited by P in both IN and OUT-patch.

3.2. P partitioning during the peak of the SERIES bloom

Since particulate P has been measured as TPP in past studies (e.g. Yoshimura et al., 2014), this is the first report to demonstrate partitioning of consumed SRP into POP_{op}, PIP_{op}, and DOP_{op} during the growth phase of a bloom. Although we have no data for the P pools other than SRP in the initial stage of the SERIES bloom, we considered that data on day 15 in the OUT-patch approximate the values in the initial stage in the IN-patch. This assumption is supported by the comparable values of Chl-*a* inventories of 16.5 mg m^{-2} for 0−50 m on day 0 in the IN-patch observed by IOS and of 17.0 mg m^{-2} on day 15 in the OUT-patch observed in the present study (Fig. 2a). With this simple assumption, to estimate the net productions of P pools from the initial stage to the peak of the bloom on day 17, the values on day 15 in the OUT-patch were subtracted from those on day 17 in the IN-patch. We estimated net productions of POP_{op}, PIP_{op}, and DOP_{op} at the peak of the bloom as 4.1 ± 0.2, 1.8 ± 0.1, and 0.9 ± 0.9 mmol m^{-2}, and their proportions as 60, 27, and 13 %, respectively. Our data show that POP_{op} and PIP_{op} were newly produced at a ratio of 7:3. The PIP_{op} pool in phytoplankton was assumed to be composed of intracellular stored P as PO_4, pyro-, and polyphosphate

(Labry et al., 2013; Paytan et al., 2003), and adsorbed P onto phytoplankton cell surfaces (Fu et al., 2005) (Fig. 1). Note that a significant part of pyro- and polyphosphate would be measured as POP_{op}, which is basically composed of P-containing cell components such as phosphoesters and nucleotides (Fig. 1). Although a part of the P incorporated into phytoplankton cells can be converted into DOP_{op} through several possible processes of autotrophic and heterotrophic activities as described for dissolved organic C (Nagata, 2000), observed DOP_{op} production was within the range of uncertainty of analytical precision (Fig. 4d). Considering DOP/Chl-*a* production ratios during subarctic phytoplankton blooms are reported as 0.0027−0.0044 mol/g (Yoshimura et al., 2014), we confirmed that the estimated DOP production of 0.016−0.026 μmol L^{-1} under a condition of 6 μg L^{-1} of Chl-*a* production in SERIES surface waters is within the level of the precision of our DOP analyses as mentioned in section 2.3.

Note that the amount of net production of POP_{op}, PIP_{op}, and DOP_{op} (6.8 mmol m^{-2}) at the peak of the SERIES bloom did not match with the net consumption of SRP (16.8 mmol m^{-2}) even if we consider TPP sinking export flux of 2.6 mmol m^{-2} during day 3.5 to day 19.5, estimated from the data for particulate organic C sinking flux of 278 mmol m^{-2} reported in Timothy et al. (2006) and the Redfield ratio of C:P = 106:1 (Redfield et al., 1963). Net increased copepod biomass in 0–200 m in the IN-patch was estimated to be 0.25–0.54 mmol P m^{-2} using reported data on an increased C biomass of 0.6 gC m^{-2} (Tsuda et al., 2006) and C:P molar ratios of 93–204 for *Pseudocalanus* sp. (Gismervik, 1997), and does not compensate the imbalanced P budget. Lateral patch evolution and patch dilution with surrounding waters have significant impacts on materials in the IN-patch of SERIES, as also shown for another in situ Fe enrichment experiment (Law et al., 2006). Timothy et al. (2006) showed that consideration of patch expansion improves the balance of the budgets of C, N, and silicon, but was unable to show balanced budgets for them. Since similarly for P this is a likely outcome, we do not further discuss quantitative analysis on the P budget in this paper.

3.3. Uncoupled behavior of POP and PIP between before and after the peak of the SERIES bloom

After the peak of the bloom, we found that POP_{op} and PIP_{op} dynamics were not coupled. This was typically observed in the different timing of the peaks of POP_{op} (day 17; Fig. 4b) and PIP_{op} (day 19; Fig. 4c), two days later than the peak of Chl-*a* and POP_{op}. In

279 contrast to a significant correlation between POP_{op} and Chl-*a* (Spearman's rank correlation, p
280 < 0.05) during our observation period, PIP_{op} did not show a clear correlation with Chl-*a*
281 (Spearman's rank correlation, $p > 0.1$). In addition, rapid change in each proportion in the TPP
282 pool occurred between before and after the peak of the bloom (Fig. 5). While PIP_{op} in the
283 IN-patch until the peak of the bloom and OUT-patch composed 25 % of the TPP pool, the
284 proportions increased significantly (ANOVA, Tukey's test, $p < 0.01$) to 50 % on average
285 during days 19−26 in the IN-patch (Fig. 5). The uncoupled behavior of POP_{op} and PIP_{op}
286 between before and after the peak of the bloom is a highlight of this study.

287 Physiological status of phytoplankton can explain the difference in the PIP_{op}
288 proportion. Phytoplankton communities showed a relatively high net growth rate (0.2−0.3
289 day^{-1}) on days 15−17 of the IN-patch (Boyd et al., 2005) and may show a relatively high
290 growth rate in the OUT-patch due to low Fe adapted small-sized phytoplankters and closely
291 balanced algal growth-microzooplankton grazing systems in Fe limited waters, as shown in
292 Liu et al. (2002). Under these conditions, we found a similar PIP_{op} proportion of 20−30 % for
293 the IN and OUT-patch although size compositions of Chl-*a* were different with dominance of
294 > 20 μm fraction on days 15−17 of the IN-patch and of < 20 μm fraction in the OUT-patch
295 (Saito et al., 2006). Similar values for the PIP_{op} proportion of 10−20 % were observed in
296 North Pacific surface waters (Yoshimura et al., 2007), consistent with the relatively high
297 growth rate of ambient phytoplankton communities which is closely coupled with high
298 microzooplankton grazing rates (Calbet and Landry, 2004; Liu et al., 2002). On the other hand,
299 elevated PIP_{op} proportions of 50 % were observed for phytoplankton communities with a
300 depressed growth rate (0.1−0.2 day^{-1}) on days 19−26 of the IN-patch (Boyd et al., 2005),
301 although > 20 μm fraction still dominated the communities (Saito et al., 2006). Although
302 higher PIP_{op} proportions are expected to be observed toward the end of the bloom, the
303 proportion peaked on day 19 and did not further increase during the declining phase (Fig. 5).
304 This is the period of rapid decrease in TPP pools (Fig. 4a), therefore more senescent
305 phytoplankton cells with higher PIP_{op} proportion would sink out or be decomposed. PIP_{op}
306 proportions observed in the declining phase are relatively close to the proportions reported for
307 sinking particulate matter with typical values of 50−70 % (Benitez-Nelson et al., 2007; Lyons
308 et al., 2011; Paytan et al., 2003). The sinking particles were mainly composed of detritus
309 including dead phytoplankton cells. PIP_{op} proportions in phytoplankton may increase with
310 depressed growth conditions.

311 In our observation, TPP inventory was relatively stable from day 17 at which POP_{op}

peaked to day 19 at which PIP_{op} peaked (Fig. 4a), suggesting that decreased POP_{op} was replaced by PIP_{op} through intracellular P metabolisms. In phytoplankton cells, many enzymes such as alkaline phosphatase, polyphosphate kinase, and exophosphatase work to transport P between key P-containing molecules (Lin et al., 2016). If these enzymes are still active when phytoplankton growth has slowed down, the enzyme activities contribute to the remineralization of organic P compounds to PO_4. Since we must consider that POP_{op} contains polyphosphates due to an analytical restriction, production of PO_4 from polyphosphate may contribute to transform POP_{op} to PIP_{op}. This is like an intracellular autolysis of P compounds. This is reasonable to explain why P is preferentially regenerated from particulate materials relative to C and N as reported in past studies (Engel et al., 2002; Paytan et al., 2003; Yoshimura et al., 2009). In addition, more PO_4 is scavenged onto phytoplankton cell surface under the growth rate depressed conditions (Fu et al., 2005), leading to increased PIP_{op} proportions. Days 17−19 represented the period with higher bacterial biomass and production, but the substantial change did not occur between the values on day 17 and day 19 when a rapid shift occurred in PIP_{op} proportions. Bacterial and zooplankton activities play roles to remineralize POP_{op}, but these should be detected as PO_4 increase, which was observed as a SRP inventory increase in our observations (Fig. 3b). Although increases in detritus concentration may change PIP_{op} proportions, no data are available to estimate the contributions of detritus in particulate matter during SERIES. Discussions of the dynamics of particulate P pools with particulate organic C and N might enable a clearer understanding of bioactive element cycles and their interactions, direct measurements of particulate organic C and N during the SERIES experiment are not available to our knowledge. We suggest that physiological status of the phytoplankton assemblage determines the POP_{op}:PIP_{op} ratio in the TPP pool.

Another plausible explanation for the changes in POP_{op}:PIP_{op} ratios other than physiological mechanisms is the floral shift in the dominant diatoms around day 17 from *Chaetoceros* spp. and *Thalassiosira* spp. to *Thalassiothrix longissima* (Boyd et al., 2005). Although different species could have different cellular POP_{op}:PIP_{op} ratios, this has not yet been fully examined. Using different P fractionation methods, Miyata et al. (1986) reported that the proportions of PIP (orthophosphate + acid-soluble polyphosphates + acid-insoluble polyphosphates) to total cellular P have a range from ca. 30 % in P limited to 40 % in N limited chemostat culture of *Skeletonema costatum* and from 24 % to 35 % in that of *Heterosigma akashiwo*, indicating relatively small interspecific difference. On the other hand,

using ^{31}P NMR spectroscopy, Cade-Menun and Paytan (2010) has reported relatively wide ranges of PIP proportion (orthophosphate + pyrophosphates + polyphosphates) to total cellular P for 12 algal species from 40 % to 82 % under optimal growth conditions with some significant change under stressed conditions. Since a direct comparison between the results from different methods is not straightforward, further data are required for the method used in this study. However note that similar POP_{op}:PIP_{op} ratios were observed between days 15−17 of the IN-patch with dominance of > 20 µm diatoms and the OUT-patch with dominance of < 20 µm phytoplankton such as *Synechococcus*, Prasinophyceae, and Prymnesiophyceae (Marchetti et al., 2006) (Fig. 5), suggesting that different phytoplankton species and groups have a similar POP_{op}:PIP_{op} ratio under P sufficient conditions in the studied area.

4. Conclusion

We found uncoupling of POP_{op} and PIP_{op} dynamics during the peak and decline phase of the phytoplankton bloom. POP_{op}:PIP_{op} ratio of suspended particulate matter may be a key factor to understand subsequent P regeneration. In this regard, characterization of the composition of PIP_{op} (PO_4 or polyphosphates) will enable a clearer understanding of P biogeochemistry. TPP fractionation provides powerful insights to better understand the marine P cycle. In addition, interspecific differences in cellular POP_{op}:PIP_{op} ratio and changes in the ratio during different growth stages of the phytoplankton from exponential growth through stationary to decline phase should be clarified in future comprehensive studies including culture experiments. Recent development of a sensitive analytical method for the fractionations of POP_{op} and PIP_{op} reported by Ehama et al. (2016) will enable further progress this research field.

Acknowledgments

We acknowledge the field assistance of the captain, officers, crew, and scientists aboard the *Kaiyo-Maru*. We thank Institute of Ocean Sciences, Fisheries and Oceans Canada for the usage of Chl-*a* and SRP data, K. Sugita for the assistance in the laboratory on land, C. Norman for his help to improve the English of the manuscript. This work was supported by a grant from CRIEPI (U00024).

References

Aoyama, M., Ota, H., Kimura, M., Kitao, T., Mitsuda, H., Murata, A., Sato, K., 2012. Current status of homogeneity and stability of the reference materials for nutrients in seawater. Anal. Sci. 28, 911–916.

Asahi, T., Ichimi, K., Yamaguchi, H., Tada, K., 2014. Horizontal distribution of particulate matter and its characterization using phosphorus as an indicator in surface coastal water, Harima-Nada, the Seto Inland Sea, Japan. J. Oceanogr. 70, 277–287.

Aspila, K.I., Agemian, H., Chau, A.S.Y., 1976. A semi-automated method for the determination of inorganic, organic and total phosphate in sediments. Analyst 101, 187–197.

Baldwin, D.S., 1998. Reactive “organic” phosphorus revisited. Wat. Res. 32, 2265–2270.

Benitez-Nelson, C., O'Neill, L., Kolowith, L.C., Pellechia, P., Thunell, R., 2004. Phosphonates and particulate organic phosphorus cycling in an anoxic marine basin. Limnol. Oceanogr. 49, 1593–1604.

Benitez-Nelson, C.R., 2000. The biogeochemical cycling of phosphorus in marine systems. Earth-Sci. Rev. 51, 109–135.

Benitez-Nelson, C.R., O'Neill Madden, L.P., Styles, R.M., Thunell, R.C., Astor, Y., 2007. Inorganic and organic sinking particulate phosphorus fluxes across the oxic/anoxic water column of Cariaco Basin, Venezuela. Mar. Chem. 105, 90–100.

Biddanda, B., Benner, R., 1997. Carbon, nitrogen, and carbohydrate fluxes during the production of particulate and dissolved organic matter by marine phytoplankton. Limnol. Oceanogr. 42, 506–518.

Björkman, K.M., Karl, D.M., 2003. Bioavailability of dissolved organic phosphorus in the euphotic zone at Station ALOHA, North Pacific Subtropical Gyre. Limnol. Oceanogr. 48, 1049–1057.

Boyd, P., Law, C., Wong, C., Nojiri, Y., Tsuda, A., Levasseur, M., Takeda, S., Rivkin, R., Harrison, P., Strzepek, R., Gower, J., McKay, R., Abraham, E., Arychuk, M., Barwell-Clarke, J., Crawford, W., Hale, M., Harada, K., Johnson, K., Kiyosawa, H., Kudo, I., Marchetti, A., Miller, W., Needoba, J., Nishioka, J., Ogawa, H., Page, J., Robert, M., Saito, H., Sastri, A., Sherry, N., Soutar, T., Sutherland, N., Taira, Y., Whitney, F., Wong, S.-K., Yoshimura, T., 2004. The decline and fate of an iron-induced subarctic phytoplankton bloom. Nature 428, 549–553.

Boyd, P.W., Strzepek, R., Takeda, S., Jackson, G., Wong, C., McKay, R., Law, C., Kiyosawa, H., Saito, H., Sherry, N., 2005. The evolution and termination of an iron-induced mesoscale bloom in the northeast subarctic Pacific. Limnol. Oceanogr. 50, 1872–1886.

Cade-Menun, B.J., Paytan, A., 2010. Nutrient temperature and light stress alter phosphorus and carbon forms in culture-grown algae. Mar. Chem. 121, 27–36.

Calbet, A., Landry, M.R., 2004. Phytoplankton growth, microzooplankton grazing, and carbon cycling in marine systems. Limnol. Oceanogr. 49, 51–57.

Carlson, C.A., Hansell, D.A., Peltzer, E.T., Smith Jr, W.O., 2000. Stocks and dynamics of dissolved and particulate organic matter in the southern Ross Sea, Antarctica. Deep-Sea Res. II 47, 3201–3225.

Dyhrman, S.T., 2016. Nutrients and their acquisition: phosphorus physiology in microalgae, in: Borowitzka, A.M., Beardall, J., Raven, A.J. (Eds.), The Physiology of Microalgae. Springer International Publishing, Cham, pp. 155–183.

Ehama, M., Hashihama, F., Kinouchi, S., Kanda, J., Saito, H., 2016. Sensitive determination of total particulate phosphorus and particulate inorganic phosphorus in seawater using liquid waveguide spectrophotometry. Talanta 153, 66–70.

Engel, A., Goldthwait, S., Passow, U., Alldredge, A., 2002. Temporal decoupling of carbon

426 and nitrogen dynamics in a mesocosm diatom bloom. Limnol. Oceanogr. 47, 753–
427 761.
428 Fu, F.X., Zhang, Y., Leblanc, K., Sanudo-Wilhelmy, S.A., Hutchins, D.A., 2005. The
429 biological and biogeochemical consequences of phosphate scavenging onto
430 phytoplankton cell surfaces. Limnol. Oceanogr. 50, 1459–1472.
431 Gismervik, I., 1997. Stoichiometry of some marine planktonic crustaceans. J. Plank. Res. 19,
432 279–285.
433 Hale, M.S., Rivkin, R.B., Matthews, P., Agawin, N.S.R., Li, W.K.W., 2006. Microbial
434 response to a mesoscale iron enrichment in the NE subarctic Pacific: Heterotrophic
435 bacterial processes. Deep-Sea Res. II 53, 2231–2247.
436 Hansen, H.P., Koroleff, F., 1999. Determination of nutrients, in: Grasshoff, K., Kremling, K.,
437 Ehrhardt, M. (Eds.), Methods of Seawater Analysis, Third Edition. Wiley-VCH
438 Verlag GmbH, Weinheim, Germany, pp. 159–228.
439 Holm-Hansen, O., Lorenzen, C.J., Holmes, R.W., Strickland, J.D.H., 1965. Fluorometric
440 determination of chlorophyll. Journal du Conseil 30, 3–15.
441 Karl, D., 2014. Microbially mediated transformations of phosphorus in the sea: New views of
442 an old cycle. Annu. Rev. Mar. Res. 6, 279–337.
443 Karl, D.M., Björkman, K.M., 2015. Dynamics of DOP, in: Hansell, D.A., Carlson, C.A. (Eds.),
444 Biogeochemistry of Marine Dissolved Organic Matter. Academic Press, San Diego,
445 pp. 233–334.
446 Kolowith, L.C., Ingall, E.D., Benner, R., 2001. Composition and cycling of marine organic
447 phosphorus. Limnol. Oceanogr. 46, 309–320.
448 Labry, C., Youenou, A., Delmas, D., Michelon, P., 2013. Addressing the measurement of
449 particulate organic and inorganic phosphorus in estuarine and coastal waters. Cont.
450 Shelf Res. 60, 28–37.
451 Law, C.S., Crawford, W.R., Smith, M.J., Boyd, P.W., Wong, C.S., Nojiri, Y., Robert, M.,
452 Abraham, E.R., Johnson, W.K., Forsland, V., Arychuk, M., 2006. Patch evolution and
453 the biogeochemical impact of entrainment during an iron fertilisation experiment in
454 the sub-Arctic Pacific. Deep-Sea Res. II 53, 2012–2033.
455 Lin, P., Guo, L., Chen, M., Cai, Y., 2013. Distribution, partitioning and mixing behavior of
456 phosphorus species in the Jiulong River estuary. Mar. Chem. 157, 93–105.
457 Lin, P., Guo, L., Chen, M., Tong, J., Lin, F., 2012. The distribution and chemical speciation of
458 dissolved and particulate phosphorus in the Bering Sea and the Chukchi–Beaufort
459 Seas. Deep-Sea Res. II 81–84, 79–94.
460 Lin, S., Litaker, R.W., Sunda, W.G., 2016. Phosphorus physiological ecology and molecular
461 mechanisms in marine phytoplankton. J. Phycol. 52, 10–36.
462 Liu, H., Suzuki, K., Saino, T., 2002. Phytoplankton growth and microzooplankton grazing in
463 the subarctic Pacific Ocean and the Bering Sea during summer 1999. Deep-Sea Res.
464 I 49, 363–375.
465 Loh, A.N., Bauer, J.E., 2000. Distribution, partitioning and fluxes of dissolved and particulate
466 organic C, N and P in the eastern North Pacific and Southern Oceans. Deep-Sea Res.
467 I 47, 2287–2316.
468 Lyons, G., Benitez-Nelson, C.R., Thunell, R.C., 2011. Phosphorus composition of sinking
469 particles in the Guaymas Basin, Gulf of California. Limnol. Oceanogr. 56, 1093–
470 1105.
471 Marchetti, A., Sherry, N.D., Kiyosawa, H., Tsuda, A., Harrison, P.J., 2006. Phytoplankton
472 processes during a mesoscale iron enrichment in the NE subarctic Pacific: Part
473 I—Biomass and assemblage. Deep-Sea Res. II 53, 2095–2113.
474 Miyata, K., Hattori, A., 1986. A simple fractionation method for determination of phosphorus
475 components in phytoplankton: Application to natural populations of phytoplankton in

summer surface waters of Tokyo Bay. J. Oceanogr. Soc. Japan 42, 255–265.
Miyata, K., Hattori, A., Ohtsuki, A., 1986. Variation of cellular phosphorus composition of *Skeletonema costatum* and *Heterosigma akashiwo* grown in chemostats. Mar. Biol. 93, 291–297.
Nagata, T., 2000. Production mechanisms of dissolved organic matter, in: Kirchmann, D.L. (Ed.), Microbial Ecology of the Oceans. Wiley-Liss, New York, NY, pp. 121–152.
Paytan, A., Cade-Menun, B.J., McLaughlin, K., Faul, K.L., 2003. Selective phosphorus regeneration of sinking marine particles: evidence from ^{31}P-NMR. Mar. Chem. 82, 55–70.
Piper, M.M., Benitez-Nelson, C.R., Frey, K.E., Mills, M.M., Pal, S., 2016. Dissolved and particulate phosphorus distributions and elemental stoichiometry throughout the Chukchi Sea. Deep-Sea Res. II 130, 76–87.
Redfield, A.C., Ketchum, B.H., Richards, F.A., 1963. The influence of organisms on the composition of seawater, in: Hill, M.N. (Ed.), The Sea. Wiley Interscience, New York, pp. 26–77.
Ridal, J.J., Moore, R.M., 1990. A re-examination of the measurement of dissolved organic phosphorus in seawater. Mar. Chem. 29, 19–31.
Ruttenberg, K.C., 1992. Development of a sequential extraction method for different forms of phosphorus in marine sediments. Limnol. Oceanogr. 37, 1460–1482.
Saito, H., Tsuda, A., Nojiri, Y., Nishioka, J., Takeda, S., Kiyosawa, H., Kudo, I., Noiri, Y., Ono, T., Taira, Y., Suzuki, K., Yoshimura, T., Boyd, P.W., 2006. Nutrient and phytoplankton dynamics during the stationary and declining phases of a phytoplankton bloom induced by iron-enrichment in the eastern subarctic Pacific. Deep-Sea Res. II 53, 2168–2181.
Solórzano, L., Sharp, J.H., 1980. Determination of total dissolved phosphorus and particulate phosphorus in natural waters. Limnol. Oceanogr. 25, 754–758.
Thomson-Bulldis, A., Karl, D., 1998. Application of a novel method for phosphorus determinations in the oligotrophic North Pacific Ocean. Limnol. Oceanogr. 43, 1565–1577.
Timothy, D.A., Wong, C.S., Nojiri, Y., Ianson, D.C., Whitney, F.A., 2006. The effects of patch expansion on budgets of C, N and Si for the Subarctic Ecosystem Response to Iron Enrichment Study (SERIES). Deep-Sea Res. II 53, 2034–2052.
Tsuda, A., Saito, H., Nishioka, J., Ono, T., Noiri, Y., Kudo, I., 2006. Mesozooplankton response to iron enrichment during the diatom bloom and bloom decline in SERIES (NE Pacific). Deep-Sea Res. II 53, 2281–2296.
Wetz, M.S., Wheeler, P.A., 2003. Production and partitioning of organic matter during simulated phytoplankton blooms. Limnol. Oceanogr. 48, 1808–1817.
Yoshimura, T., 2013. Appropriate bottles for storing seawater samples for dissolved organic phosphorus (DOP) analysis: A step towards the development of DOP reference materials. Limnol. Oceanogr.: Methods 11, 239−246.
Yoshimura, T., Nishioka, J., Ogawa, H., Kuma, K., Saito, H., Tsuda, A., 2014. Dissolved organic phosphorus production and decomposition during open ocean diatom blooms in the subarctic Pacific. Mar. Chem. 165, 46–54.
Yoshimura, T., Nishioka, J., Saito, H., Takeda, S., Tsuda, A., Wells, M., 2007. Distributions of particulate and dissolved organic and inorganic phosphorus in North Pacific surface waters. Mar. Chem. 103, 112–121.
Yoshimura, T., Ogawa, H., Imai, K., Aramaki, T., Nojiri, Y., Nishioka, J., Tsuda, A., 2009. Dynamics and elemental stoichiometry of carbon, nitrogen, and phosphorus in particulate and dissolved organic pools during a phytoplankton bloom induced by in situ iron enrichment in the western subarctic Pacific (SEEDS-II). Deep-Sea Res. II

526 56, 2863–2874.
527 Yoshimura, T., Sharp, J.H., 2010. Additional calibration of nutrient reference materials for
528 dissolved organic carbon, nitrogen, and phosphorus, in: Aoyama, M. (Ed.),
529 Comparability of Nutrients in The World's Ocean. Mother Tank, Tsukuba, Japan, pp.
530 91–100.
531 Young, C., Ingall, E., 2010. Marine dissolved organic phosphorus composition: Insights from
532 samples recovered using combined electrodialysis/reverse osmosis. Aquat. Geochem.
533 16, 563–574.

534 Figure Legends

535 Fig. 1. A diagram of the differentiations of typical P compounds into conceptually and
536 operationally defined P pools. Positions of each component among the operationally defined P
537 pools are approximately illustrated with reference to Labry et al. (2013) for particulate P and
538 to Baldwin (1998) and Thomson-Bulldis and Karl (1998) for dissolved P.

539

540 Fig. 2. Temporal variations in the vertical profiles for selected sampling days of chlorophyll-*a*,
541 particulate P, and dissolved P in the Fe enriched patch. Mean values for duplicate analysis for
542 particulate P and triplicate analysis for dissolved P are reported. Error bars are within the
543 symbols except for DOP_{op} and are not shown for DOP_{op} to simplify the figure. The figure for
544 Chl-*a* was redrawn using the data presented in Saito et al. (2006).

545

546 Fig. 3. Temporal variations in the 0−50 m inventories for chlorophyll-*a* and soluble reactive P
547 (SRP) in the IN-patch and OUT-patch. Chl-*a* and SRP data during day 0 to day 14 are
548 provided by Institute of Ocean Sciences, Fisheries and Oceans Canada (F.A. Whitney,
549 Personal communication). The data in gray background during day 15 to day 26 was obtained
550 in our study. Chl-*a* inventory was calculated based on the data presented in Saito et al. (2006).

551

552 Fig. 4. Temporal variations in the 0−50 m inventories for the particulate P and dissolved
553 organic P (DOP_{op}) in the IN-patch and OUT-patch. Integrated values were calculated using
554 results of each depth (mean ± range of duplicate analysis for particulate P and mean ± 1
555 standard deviation of triplicate analysis for DOP_{op}). Error bars are within the symbols except
556 for DOP_{op}.

557

558 Fig. 5. Temporal variations in the relative composition of fractionated particulate P in the
559 0−50 m inventories for the IN-patch and OUT-patch.

Fig. 1

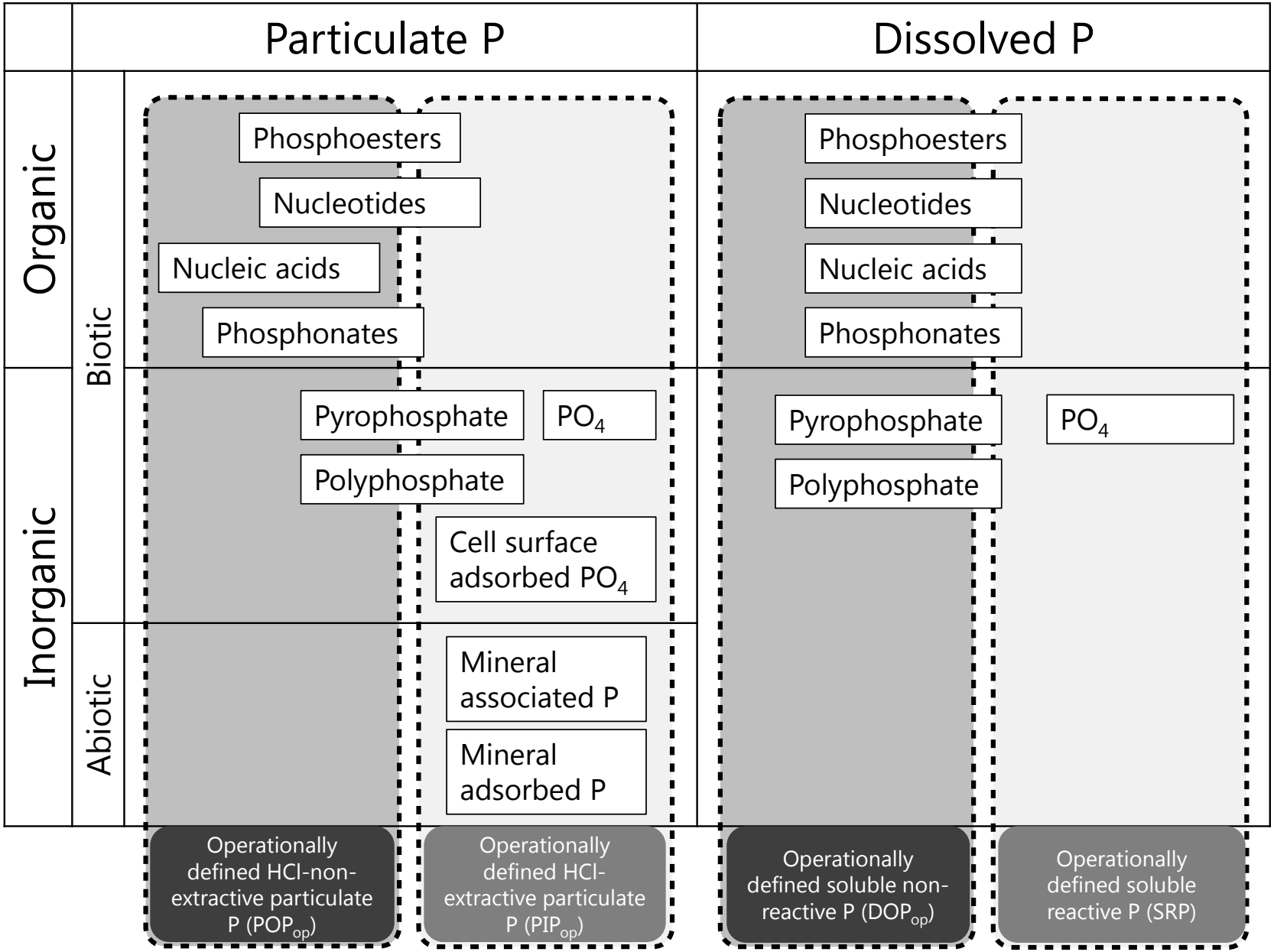
Particulate P
Dissolved P
Organic
Inorganic
Biotic
Abiotic
Phosphoesters
Nucleotides
Nucleic acids
Phosphonates
Pyrophosphate
PO4
Polyphosphate
Cell surface adsorbed PO4
Mineral associated P
Mineral adsorbed P
Phosphoesters
Nucleotides
Nucleic acids
Phosphonates
Pyrophosphate
PO4
Polyphosphate
Operationally defined HCl-non-extractive particulate P (POPop)
Operationally defined HCl-extractive particulate P (PIPop)
Operationally defined soluble non-reactive P (DOPop)
Operationally defined soluble reactive P (SRP)

Fig.2

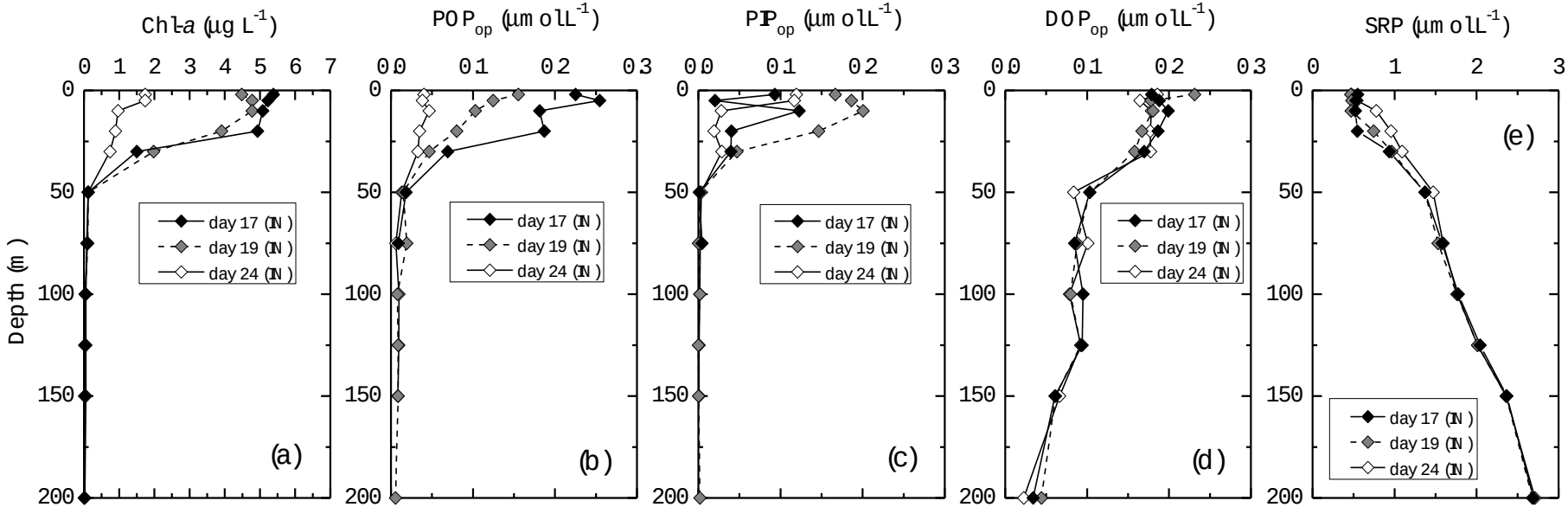
Chl-a (μg L-1)
POPop (μmol L-1)
PIPop (μmol L-1)
DOPop (μmol L-1)
SRP (μmol L-1)
Depth (m)
day 17 (IN)
day 19 (IN)
day 24 (IN)
(a)
(b)
(c)
(d)
(e)

Fig.3

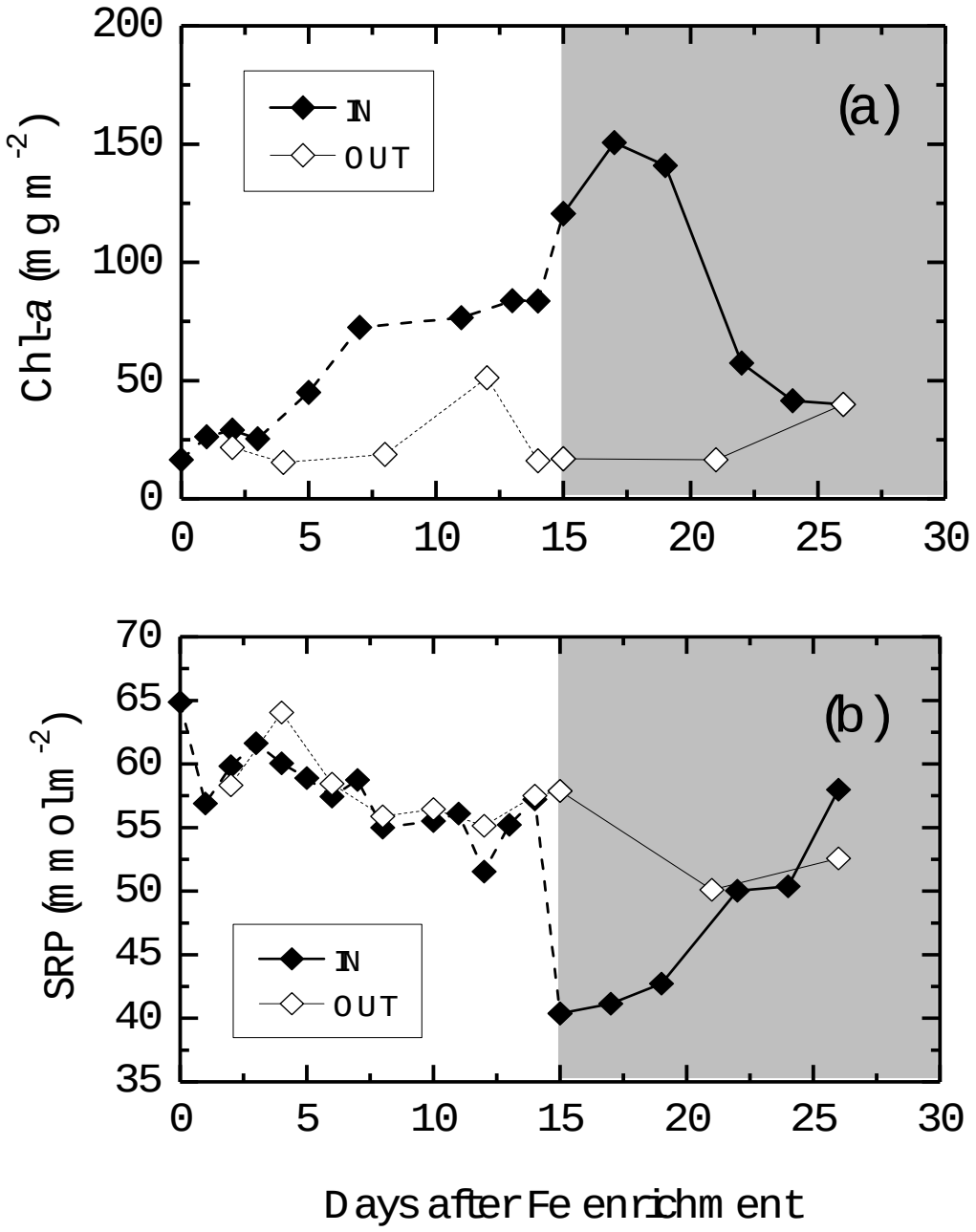
Chl-a (mg m-2)
200
150
100
50
0
IN
OUT
(a)
0
5
10
15
20
25
30
SRP (mmol m-2)
70
65
60
55
50
45
40
35
IN
OUT
(b)
Days after Fe enrichment

Fig.4

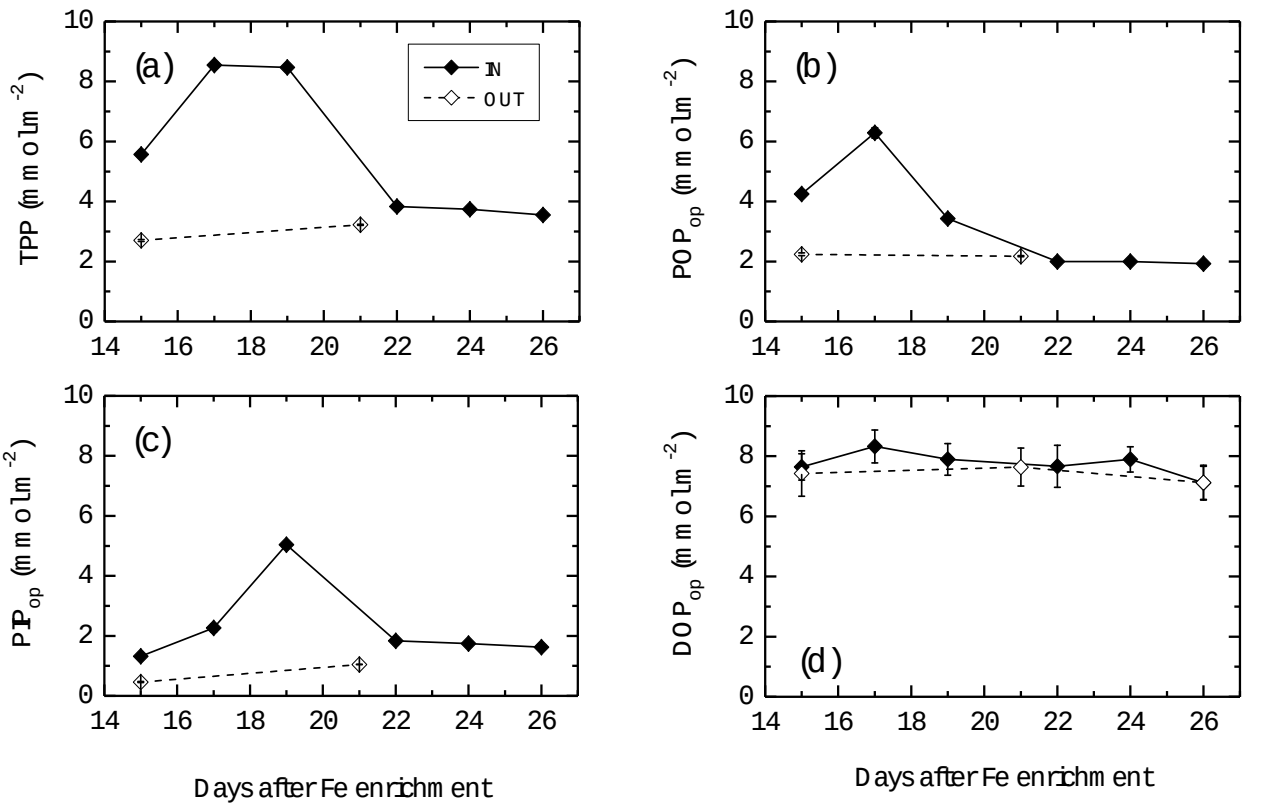
(a)
IN
OUT
TPP (mmolm-2)
(b)
POPop (mmolm-2)
(c)
PIPop (mmolm-2)
(d)
DOPop (mmolm-2)
Days after Fe enrichment
Days after Fe enrichment

Fig.5

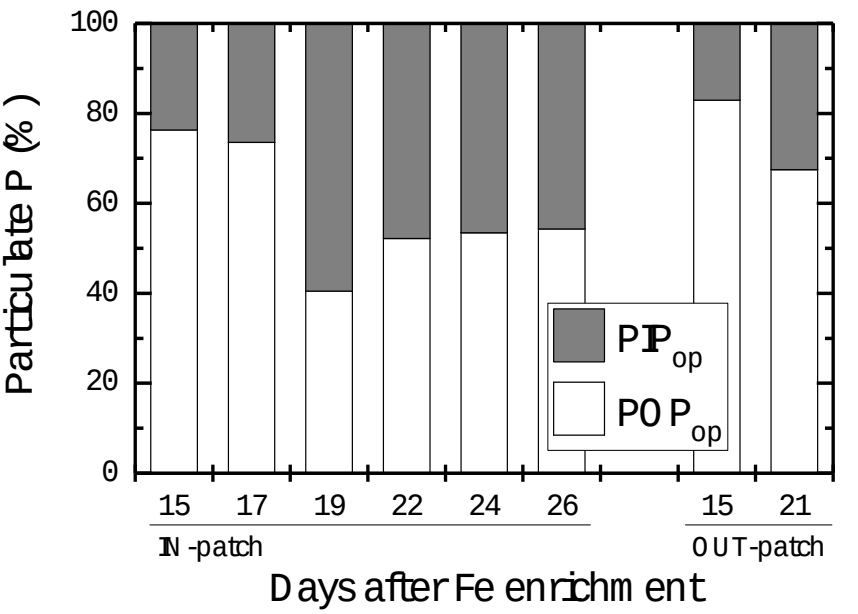
100
80
60
40
20
0
Particulate P (%)
PIP op
POP op
15
17
19
22
24
26
15
21
IN-patch
OUT-patch
Days after Fe enrichment